

AD-A141 923

UNIAXIAL DRAW OF POLY(ETHYLENE OXIDE) BY SOLID STATE
EXTRUSION(U) MASSACHUSETTS UNIV AMHERST DEPT OF POLYMER
SCIENCE AND ENGINE... B S KIM ET AL. 15 AUG 83 TR-28

1/1

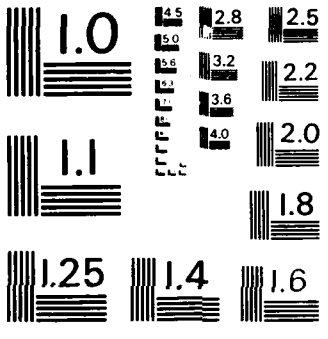
UNCLASSIFIED

N00014-83-K-0228

F/G 11/9

NL





MICROCOPY RESOLUTION TEST CHART
NATIONAL BUREAU OF STANDARDS-1963-A

12

Unclassified

AD-A141 923
DTIC FILE COPY

REPORT DOCUMENTATION PAGE		READ INSTRUCTIONS BEFORE COMPLETING FORM
1. REPORT NUMBER Technical Report No. 20	2. GOVT ACCESSION NO. AD A141 923	3. RECIPIENT'S CATALOG NUMBER
4. TITLE (and Subtitle) Uniaxial Draw of Poly(Ethylene Oxide) by Solid State Extrusion		5. TYPE OF REPORT & PERIOD COVERED Interim
		6. PERFORMING ORG. REPORT NUMBER
7. AUTHOR(s) Bong Shik Kim and Roger S. Porter		8. CONTRACT OR GRANT NUMBER(s) N00014-83-K-0228
9. PERFORMING ORGANIZATION NAME AND ADDRESS Polymer Science and Engineering University of Massachusetts Amherst, Massachusetts 01003		10. PROGRAM ELEMENT, PROJECT, TASK AREA & WORK UNIT NUMBERS
11. CONTROLLING OFFICE NAME AND ADDRESS ONR Branch Office 666 Summer Street Boston, Massachusetts 02210		12. REPORT DATE August 15, 1983
		13. NUMBER OF PAGES
14. MONITORING AGENCY NAME & ADDRESS (if different from Controlling Office)		15. SECURITY CLASS. (of this report) Unclassified
		15a. DECLASSIFICATION/DOWNGRADING SCHEDULE
16. DISTRIBUTION STATEMENT (of this Report) Approved for public release; distribution unlimited		
17. DISTRIBUTION STATEMENT (of the abstract entered in Block 20, if different from Report) DTIC ELECTE JUN 11 1984 S B		
18. SUPPLEMENTARY NOTES		
19. KEY WORDS (Continue on reverse side if necessary and identify by block number) Uniaxial Draw, Poly(Ethylene Oxide), Extrusion, Melting Properties		
20. ABSTRACT (Continue on reverse side if necessary and identify by block number) Ultradrawn filaments of poly(ethylene oxide) (PEO) have been prepared by a solid-state coextrusion in an Instron capillary rheometer. Two different molecular weights, 3.0×10^5 and 4.0×10^6 , were evaluated. Properties have been examined as a function of uniaxial draw ratio. The drawn filaments of PEO exhibit extremes of melting point, percent crystallinity, birefringence, and tensile modulus. Features of a PEO filament with a draw ratio of 32 are a 72°C DSC melting point and a crystallinity of 94.0%, both measured at a scan of $2.5^\circ\text{C min}^{-1}$. The		

DD FORM 1473
1 JAN 73

EDITION OF 1 NOV 65 IS OBSOLETE
S/N 0102-014-66011

Unclassified

84 06 11 005

SECURITY CLASSIFICATION OF THIS PAGE (When Data Entered)

Unclassified

corresponding birefringence is 3.5×10^{-2} and a Young's modulus of 3.5 GPa.

SEARCHED	INDEXED
SERIALIZED	FILED
APR 19 1964	
FBI - MEMPHIS	
A-1	

Unclassified

SECURITY CLASSIFICATION OF THIS PAGE (When Data Entered)

UNIAXIAL DRAW OF POLY(ETHYLENE OXIDE) BY SOLID STATE EXTRUSION

Bong Shik Kim and Roger S. Porter
Polymer Science and Engineering Department
Materials Research Laboratory
University of Massachusetts
Amherst, Massachusetts 01003

INTRODUCTION

Extrusion of several thermoplastics in the crystalline state has been performed over this past decade^{1,2}. A purpose of these studies has been to produce highly oriented morphologies. Despite the great interest in polymer drawing, few studies on poly(ethylene oxide) (PEO) have been reported. Kitao et.al.^{3,4} employed two different drawing methods; (1) a dry and a wet process each at different temperatures; (2) a melt spinning method. A relatively low draw ratio, 7.9; percent crystallinity and birefringence were reported.

To obtain higher draw ratios and to achieve enhanced physical properties, strands of PEO were drawn in this study by solid state coextrusion by a technique reported by Griswold et.al.⁵. PEO extrudates of high draw resulting in filaments, have been evaluated by thermal analysis, mechanical properties and by birefringence.

EXPERIMENTAL

The samples of PEO used in this study were obtained in powder form from Polyscience, Inc., Pittsburg, PA. The molecular weights, \bar{M}_v , of the poly(ethylene oxide) samples were reported to be 3.0×10^5 and 4.0×10^6 . The powders were compression molded for 20 min at 110°C and 15,000 psi into sheets of 0.2 to 0.3 mm thickness followed by cooling to ambient. At this stage atmospheric moisture was not considered a problem. Samples were extrusion-drawn using solid-state coextrusion as described earlier⁵⁻⁷. Briefly, in this process a ribbon cut from the poly(ethylene oxide) sheet is inserted into 3/8 in. diameter polyethylene billets which had been split longitudinally. This assembly was then press fit into the barrel of an Instron capillary rheometer and then pushed through conical brass dies of 20° included entrance angle. The ratio of the cross-sectional area at the top of the cone to that at the bottom of the cone provides a draw ratio up to 8. This value agrees with that calculated from the displacement of transverse marks made on the PEO ribbon at higher draw; the ratio reported here may be up to 10% lower due to differential draw between the PEO ribbon and the polyethylene billet. The higher draw ratios were obtained by drawing again the same PEO ribbons within fresh polyethylene billets. Drawing is most effectively carried out at 40°C, well below the PEO melting point. This temperature led to the highest draw ratio for PEO. The extrusion rate was $\sim 0.01 \text{ cm min}^{-1}$. Solid state extrusions at 50°C were less successful possibly due to relaxation processes.

The thermal analysis instrument used was a computerized (TADS) Perkin-Elmer DSC-2. The DSC was calibrated using ice and pure Indium. Birefringence measurements were made at room temperature using a Zeiss polarizing microscope equipped with a Zeiss calcspat tilting compensator and a white light source (5500 Å wavelength). Tensile tests were made at ambient on the drawn PEO ribbons using an Instron testing machine, model TTM, at a cross-head speed of 0.1 cm min⁻¹. The initial sample length was 50 mm. Tensile modulus was calculated as the tangent to the stress-strain curve at a strain of 0.1%.

RESULTS AND DISCUSSION

The highly-drawn PEO ribbons exhibited a range of interesting properties. The most striking result of the DSC studies is the observance of uniquely high melting points. Figure 1 shows the effect of draw ratio on the endothermic peak melting temperature at a low scanning rate of $2.5^{\circ}\text{C min}^{-1}$. The melting point increases with uniaxial draw from 65°C reaching of 72°C at a draw ratio of 32. The melting point appears not yet to have reached a limit with draw, is significantly higher than previously published for PEO. Lang et.al.⁸ have reported that an unannealed PEO melts at 65°C . Mandelkern et.al.⁹ have given a value of 66°C and Porter and Boyd¹⁰ a value of 62°C . Beech and Booth¹¹ reported a melting temperature of 69.2°C for a well-annealed, high molecular weight fraction of PEO.

Nedkov et.al.¹² have carried out DSC experiments on nascent PEO. They reported melting points for the newly-formed PEO ranging from $\sim 66^{\circ}\text{C}$ for a molecular weight of 1.75×10^6 to 70°C for a molecular weight of 7.0×10^6 . Over this molecular weight range, they found a linear relationship between molecular weight and melting temperature. However, upon second heating the melting points for their samples were found to range from slightly less than 66°C for molecular weight of 1.75×10^6 to 63°C for molecular weight of 7.0×10^6 . The high melting points for the nascent samples was ascribed to the influence of tie molecules which were thought, because of polymerization conditions, to be linking lamellae. After the initial melting it is postulated that these tie molecules were reduced.

The melting points reported here may also be compared to those predicted for an infinitely-extended-chain crystal of PEO. Buckley and Kovacs¹³ calculate a theoretical melting point of $68^{\circ}\text{C} \pm 0.4^{\circ}\text{C}$. Beech and Booth¹¹ offer a value of 76°C . This latter value was obtained by extrapolation of their data for melting point and crystallization temperature. Lang et.al.⁸ report 74°C , derived from an extrapolation of peak melting temperature changes with annealing temperature. The maximum melting point of 72.1°C obtained here, at a draw ratio of 32 thus approach values derived for a fully chain extended crystal. The increase of melting point with draw ratio is consistent with an entropy constraint in the non-crystalline regions that increase with drawing¹⁴ or alternatively viewed simply as increased crystal perfection.

The effect of heating rate on peak melting temperature for the PEO of molecular weight 3.0×10^5 is shown in Figure 2. The melting temperature observed at heating rates $< 5^{\circ}\text{C min}^{-1}$ are essentially unaffected, but melting temperature measured at higher rates increase monotonically with heating rates. Since the slopes reported in Figure 2 are independent of draw ratio, superheating effects are absent. Thus the observed heating rate effect is likely due to heat transfer rather than PEO morphology. The curvature in the plots at low draw are likely the result of annealing during slow heating. According to Clements et.al.¹⁴ and Jaffe et.al.¹⁵, in oriented polymers superheating effects are attributable to the entropic restriction on molecular chains that connect two or more crystalline regions of the same or different crystals.

The monotonic increase in crystallinity in PEO on draw is shown in Figure 3. The percent crystallinity has been calculated from the heat of fusion as

determined from the area under the fusion curve. The degree of crystallinity in percent is defined as follows¹⁶:

$$\text{fraction crystallinity} = \Delta H_1 / \Delta H_2$$

where ΔH_1 is the heat of fusion of the partially crystalline specimen and ΔH_2 the heat of fusion of the perfect crystal. The % crystallinity in this study has been computed using 1980 cal/mol for ΔH_2 of PEO^{9,17}. The highest fractional crystallinity developed in this work is 94.0%, measured at a DSC scanning rate of 2.5°C min⁻¹, which was 95.3% at a scanning rate 10°C min⁻¹, both for a PEO draw ratio of 32. These values are higher than previously reported for drawn PEO, with a previous high cited of 85%⁴.

Multiple melting peaks are also a notable characteristic of the fusion curves for drawn PEO, as shown in Figure 4. Their appearance, however, is poorly reproducible. Irregularities in the melting endotherms first appear at a draw ratio of ~8 with yet more complex peaks noted at draw ratios ≥ 20 , but with the multiple peaks always disappearing on second heating of the previously drawn PEO.

Comparable features have been reported for drawn polyethylene¹⁸⁻²⁰, except that superheating is also observed. Southern¹⁸ and Mead¹⁹ with coworkers associated dual melting peaks with the presence of both chain-folded and chain-extended crystals. Aharoni and Sibilis²⁰ associated the appearance of three melting peaks to the existence of three morphologies in the drawn extrudates.

Thermal crystallization²¹ and annealing⁸ of PEO is also known to produce multiple melting peaks. Buckley and Kovacs²¹ reported that this phenomenon can

be assigned to the melting of once-folded and extended-chain crystals, with the higher endothermic peak corresponding to the extended chains. Lang et.al.⁸ reported the lowest melting peak in PEO may be interpreted as a melting of a crystalline fraction formed by some "impurities", i.e. less regular components in fractions which tend to be rejected during primary crystallization and thus crystallize separately during annealing. The next endotherm is attributed to the primary crystallization. The third peak has been ascribed to the melting of folded-chain crystals. The dual peaks observed here in ribbons drawn up to ratio of 32 are still evident even on analysis at a heating rate $80^{\circ}\text{C min}^{-1}$, as shown in Figure 5.

Results of tensile modulus and strength, calculated from stress-strain curves, are shown in Figure 6 and 7. The tensile moduli and strengths are noted to increase with uniaxial draw. The highest tensile modulus attained is 3.5 GPa. This value far exceeds the highest previously reported value for drawn PEO fibers of 793 MPa²².

The calculation of elastic moduli for PEO crystals in the chain direction has been reported to be 4.6 - 4.9 GPa²³. In this calculation, a helical skeleton conformation model of PEO is used in which the internal rotation angles are taken to be all gauche. Sakurada²⁴ obtained an estimated maximum elastic modulus of 7.8 - 9.2 GPa for the crystal lattice of PEO in which the internal rotation angles were taken to be in trans-trans-gauche conformations.

The tensile moduli of the drawn PEO measured here and reported²⁵ are insensitive to choice of molecular weight. This is similar to the result of

Perkins et.al.²⁶ in which the Young's modulus for drawn high density polyethylene is essentially independent of molecular weight.

Figure 7 shows the change of PEO tensile strength with draw ratio. Here the tensile strength of high molecular weight PEO is much higher than that for the lower. This is also consistent with results on other polymers and in accordance with the following proposal of Flory²⁷

$$\sigma = A - \frac{B}{\bar{M}_n}$$

where σ is tensile strength and the constants A and B vary with polymer composition and \bar{M}_n is the number-average molecular weight.

Birefringence has been chosen to evaluate the extent of orientation achieved on drawing by solid state extrusion. The total birefringence Δn_T of the extrudates was estimated from the equation²⁸:

$$\Delta n_T = \frac{R}{d} \cdot \lambda$$

where d is the sample thickness, R is the retardation and λ the wavelength. As shown in Figure 8, birefringence increases steeply with draw at low values, but above a draw ratio of 16, Δn_T approaches a plateau²⁹. The highest value of birefringence attained here is 3.5×10^{-2} . This is higher, but within precision of the highest prior report of 3.4×10^{-2} , for drawn PEO fiber⁴. The birefringence measured on extrudates prepared at faster extrusion rates is higher than at low. This is likely related to more annealing at lower extrusion rates for the drawn ribbon on exiting the die at 40°C and without tension³⁰.

ACKNOWLEDGEMENTS

This work was supported in part by the Office of Naval Research. B.S. Kim also wishes to acknowledge support given by the Ministry of Education, Korea, during the period of this research.

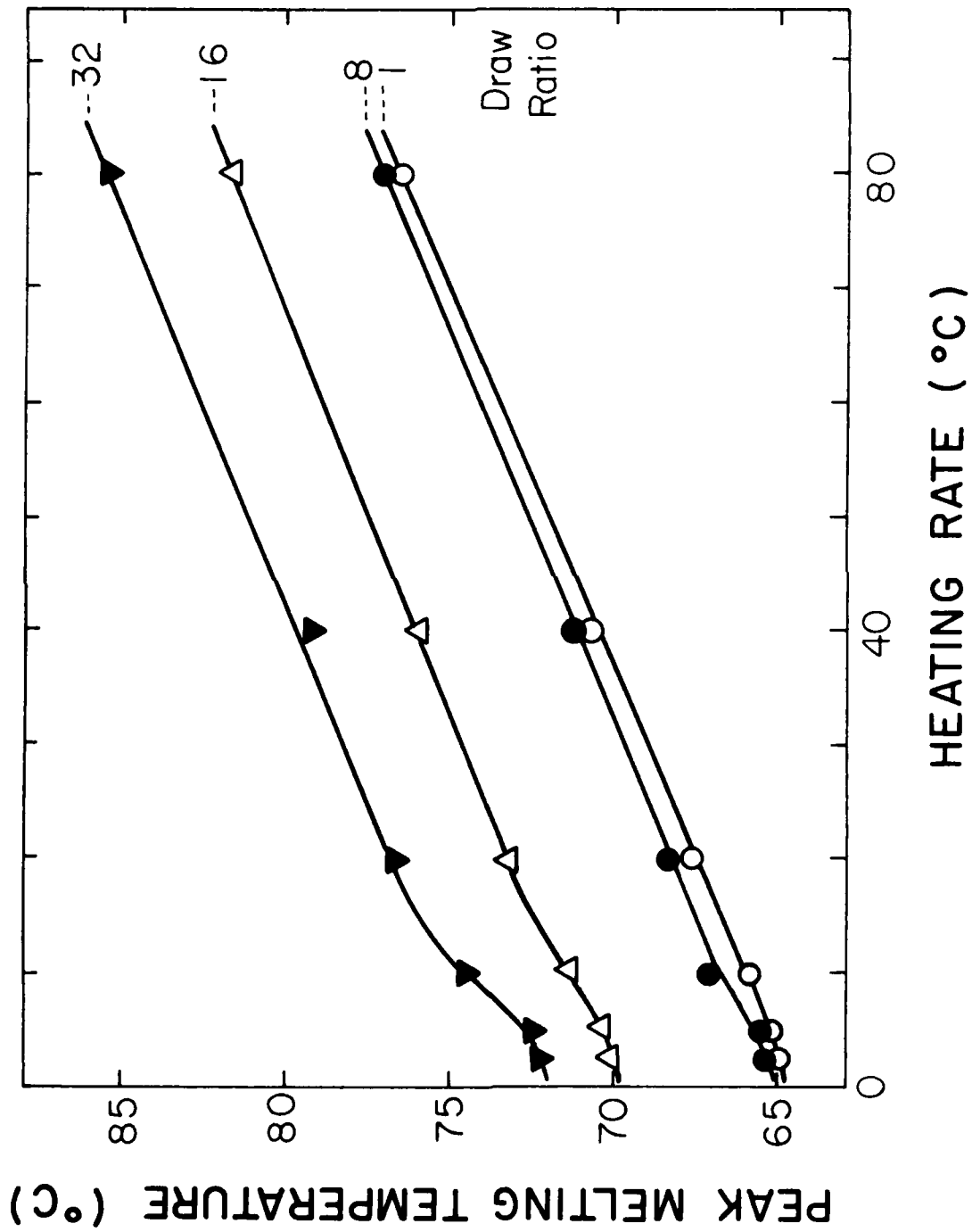
REFERENCES

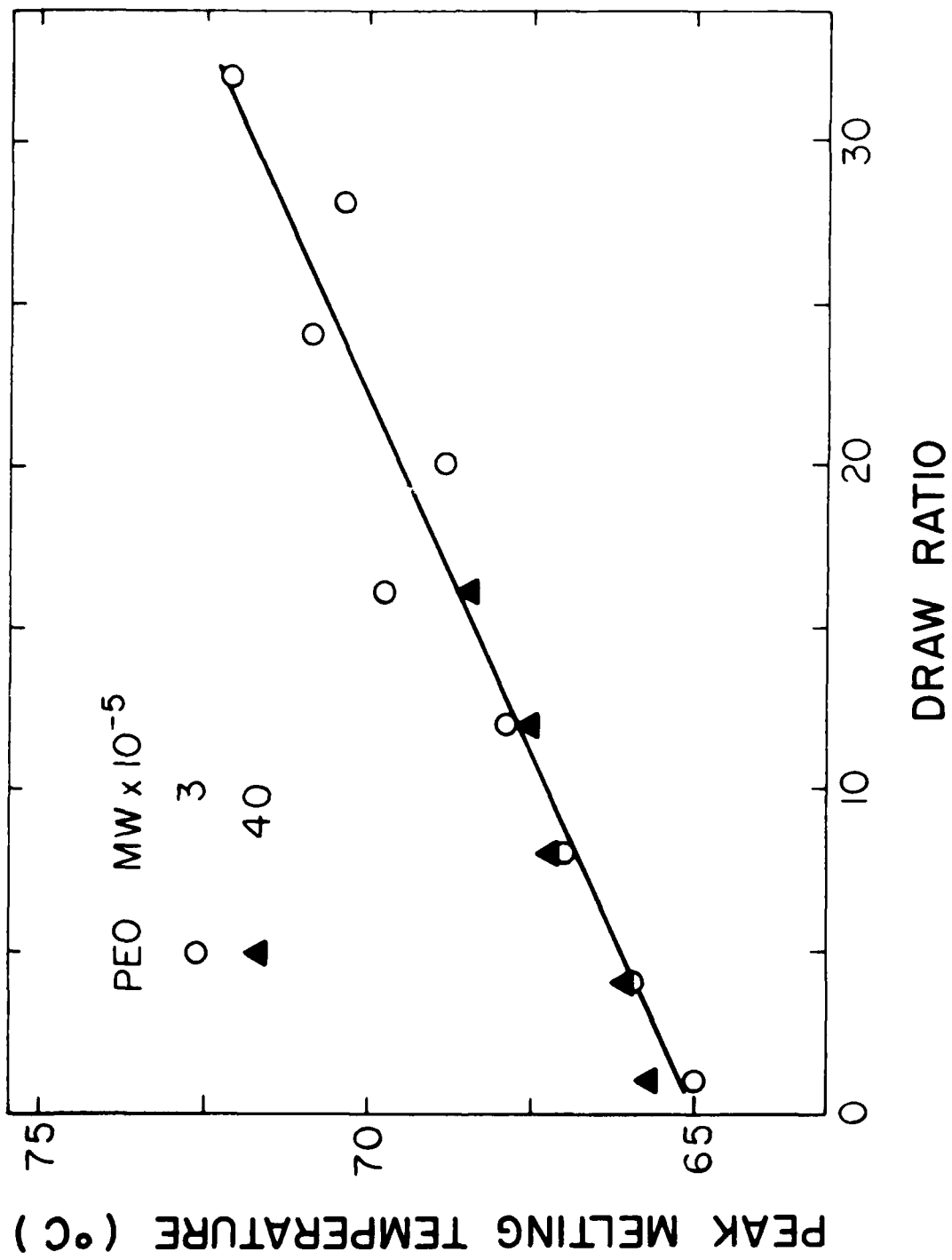
1. N.J. Capiati, S. Kojima, W.G. Perkins and R.S. Porter, J. Mater. Sci., 12, 334 (1977).
2. H. Ulrich, "Introduction to Industrial Polymers", Hanser, New York (1981).
3. T. Kitao, K. Yamada, T. Yamazaki and S. Oya, Sen-I Gakkaishi, 28, 61 (1972).
4. T. Kitao, K. Yamada, T. Yamazaki and S. Oya, Sen-I Gakkaishi, 28, 221 (1972).
5. P.D. Griswold, A.E. Zachariades and R.S. Porter, Polym. Eng. Sci., 18, 861 (1978).
6. A.E. Zachariades, W.T. Mead and R.S. Porter, Ultra-High Modulus Polymers, A. Ciferri and I.M. Ward, Editors, Applied Science Publ., Essex, England, pp. 77-116 (1979).
7. A.E. Zachariades, E.S. Sherman and R.S. Porter, J. Polym. Sci. Polym. Lett. Ed., 17, 255 (1979).
8. M.C. Lang, C. Noel and A.P. Legrand, J. Polym. Sci. Polym. Phys. Ed., 15, 1319 (1977).
9. L. Mandelkern, F.A. Quinn and P.J. Flory, J. Appl. Phys., 25, 830 (1954).
10. C.H. Porter and R.H. Boyd, Macromolecules, 4, 589 (1971).
11. D.B. Beech and C. Booth, J. Polym. Sci., B, 8, 731 (1970).
12. E. Nedkov, M. Kresteva, M. Mihailov and U. Todorova, J. Macromol. Sci., Phys., B21, 371 (1982).
13. C.P. Buckley and A.J. Kovacs, Prog. Colloid. Polym. Sci., 58, 44 (1975).

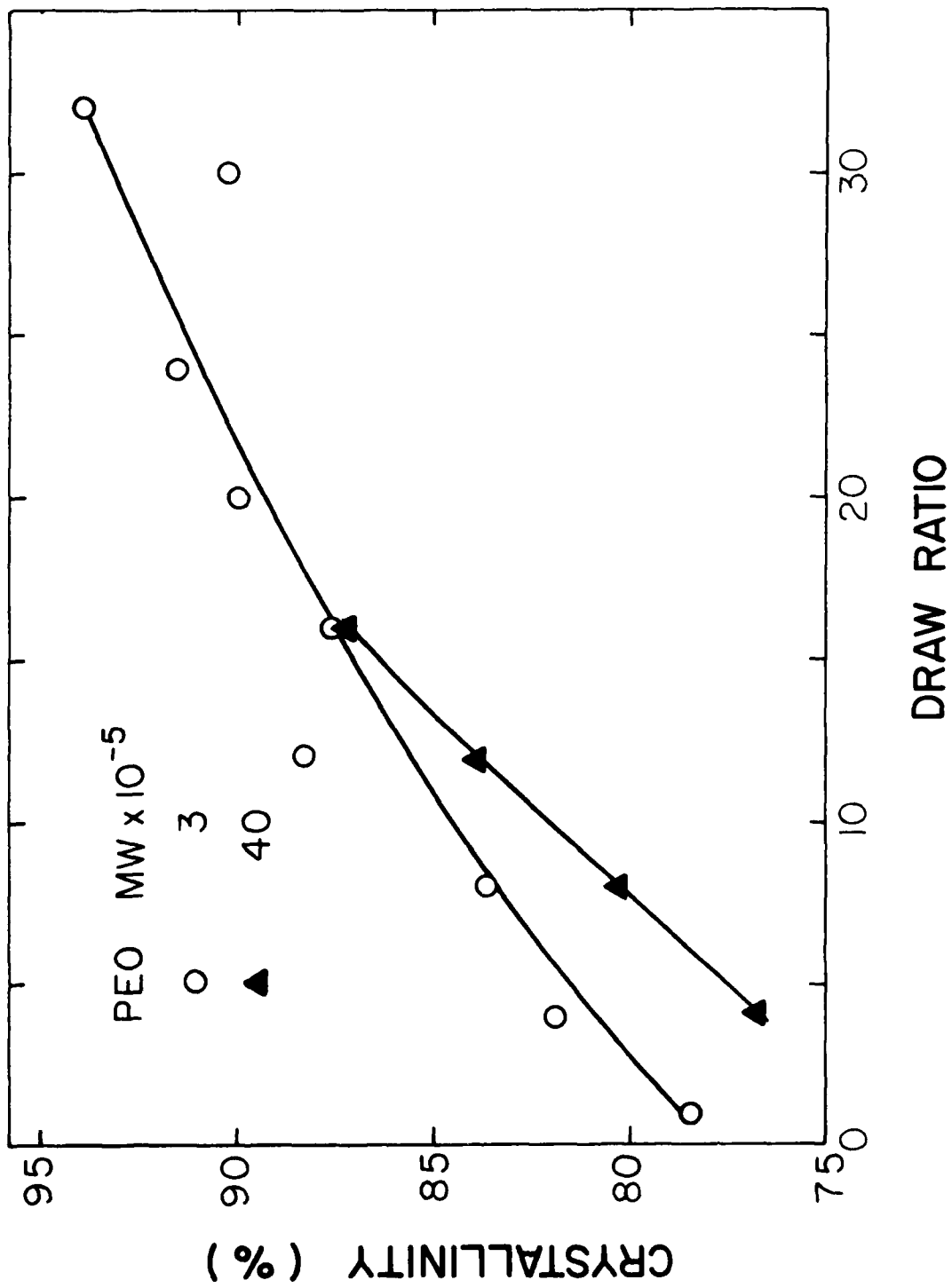
14. J. Clements, G. Capaccio and I.M. Ward, J. Polym. Sci. Polym. Phys. Ed., 7, 693 (1979).
15. M. Jaffe and B. Wunderlich, "Thermal Physics", Vol. 17, R.F. Schwenker and P.D. Garm, Editors, Academic Press, New York (1969).
16. P. Meares, "Polymers: Structure and Bulk Properties", Van Nostrand Reinhold, London (1965).
17. L. Mandelkern, J. Appl. Phys., 26, 443 (1955).
18. J.H. Southern and R.S. Porter, J. Macromol. Sci. Phys., B4, 541 (1970).
19. W.T. Mead and R.S. Porter, Intern. J. Polym. Mater., 7, 29 (1979).
20. S.M. Aharoni and J.P. Sibilias, J. Appl. Polym. Sci., 23, 133 (1979); Polym. Eng. Sci. 19, 450 (1979).
21. C.P. Buckley and A.J. Kovacs, Colloid and Polymer Sci., 254, 695 (1976).
22. W.A. Miller, R.G. Shaw and P.A. King, U.S. Patent, 3,941,865.
23. S. Enomoto and M. Asahina, J. Polym. Sci., 59, 113 (1962).
24. I. Sakurada, T. Ito and K. Nakamae, J. Polym. Sci., C15, 175 (1966).
25. D.C. Bassett, "Principles of Polymer Morphology", Cambridge University Press, England (1981).
26. W.G. Perkins and R.S. Porter, Polym. Eng. Sci., 16, 200 (1976).
27. P.J. Flory, J. Amer. Chem. Soc., 67, 2048 (1945).
28. G.L. Wilkes, J. Macromol. Sci. Chem., C10, 149 (1974).
29. I.M. Ward, "Mechanical Properties of Solid Polymers", Wiley, London (1971).
30. G. Capaccio, T.A. Crompton and I.M. Ward, J. Polym. Sci. Polym. Phys. Ed., 18, 301 (1980).

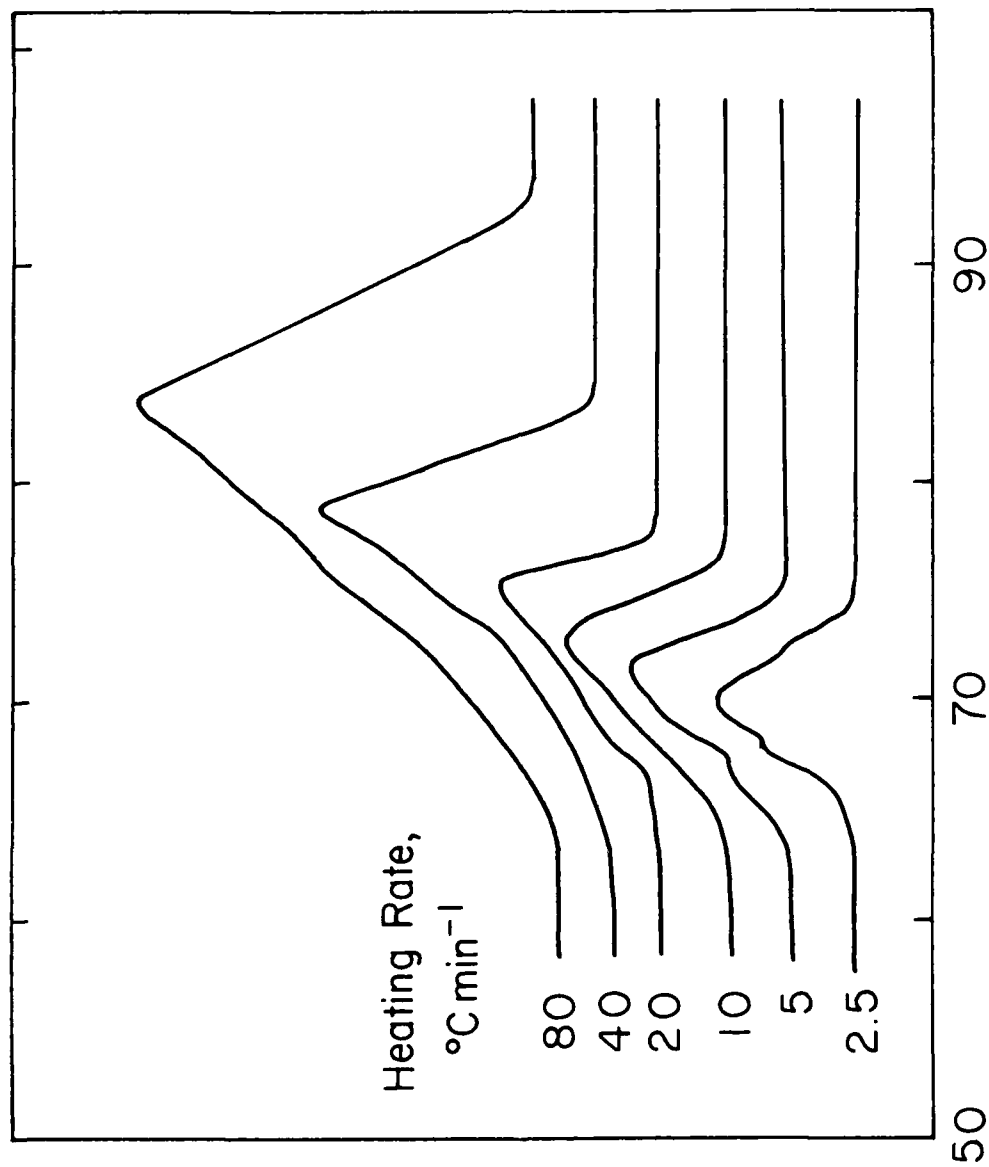
FIGURE CAPTIONS

- FIGURE 1: Effect of draw ratio on the peak melting temperature at a heating rate of $2.5^{\circ}\text{C min}^{-1}$. PEO drawn at 40°C : \circ : $\bar{M}_v = 3.0 \times 10^5$; \blacktriangle : $\bar{M}_v = 4.0 \times 10^6$.
- FIGURE 2: Effect of heating rate on the peak melting temperature of undrawn film and drawn films of PEO $\bar{M}_v = 3.0 \times 10^5$.
- FIGURE 3: Effect of draw ratio on the percent crystallinity of PEO at a heating rate of $2.5^{\circ}\text{C min}^{-1}$.
- FIGURE 4: DSC endotherm observed at indicated draw ratio measured at a heating rate of $2.5^{\circ}\text{C min}^{-1}$. $\bar{M}_v = 3 \times 10^5$.
- FIGURE 5: Endotherm for PEO ribbons of draw ratio 32 observed at indicated heating rates. $\bar{M}_v = 3.0 \times 10^5$.
- FIGURE 6: PEO tensile modulus as a function of draw ratio.
- FIGURE 7: PEO tensile strength as a function of draw ratio.
- FIGURE 8: Birefringence of uniaxially drawn PEO film. \circ : $\bar{M}_v = 3.0 \times 10^5$ and extrusion rate 0.01 cm min^{-1} , \bullet : $\bar{M}_v = 3.0 \times 10^5$ and extrusion rate 0.1 cm min^{-1} , \blacktriangle : $\bar{M}_v = 4.0 \times 10^6$ and extrusion rate 0.01 cm min^{-1} .





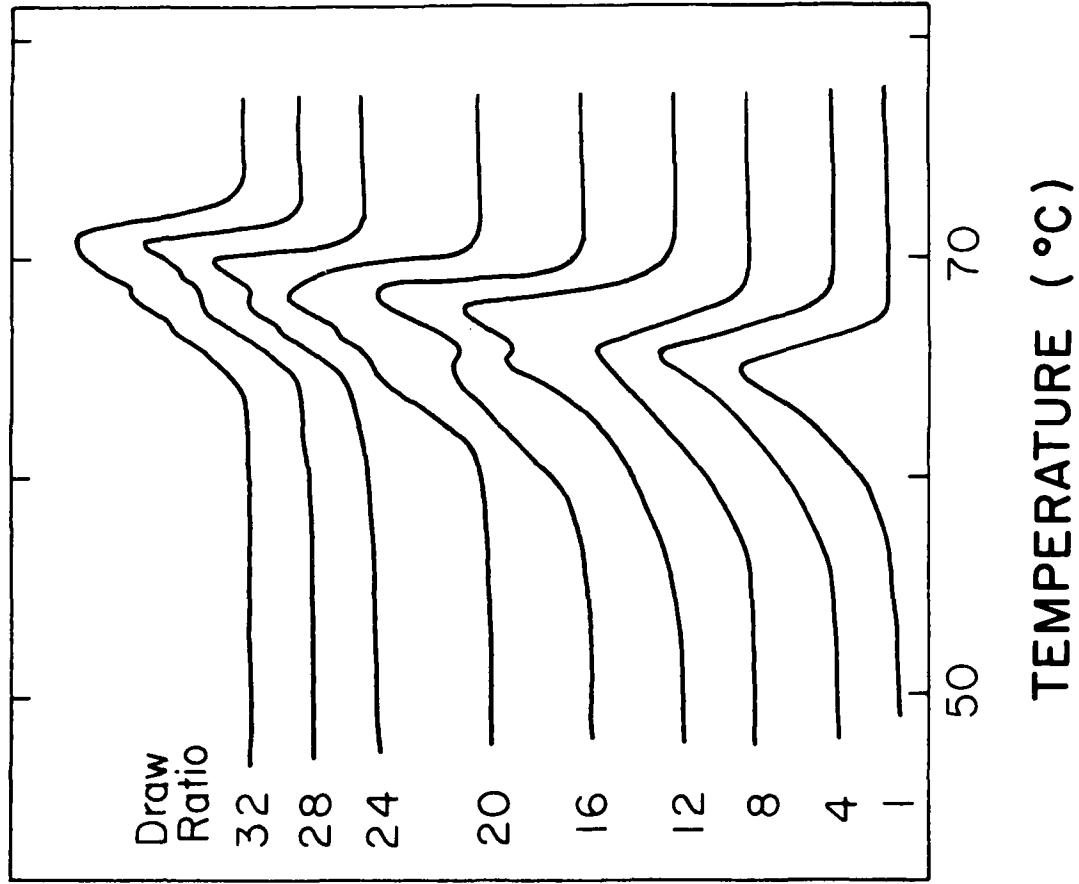


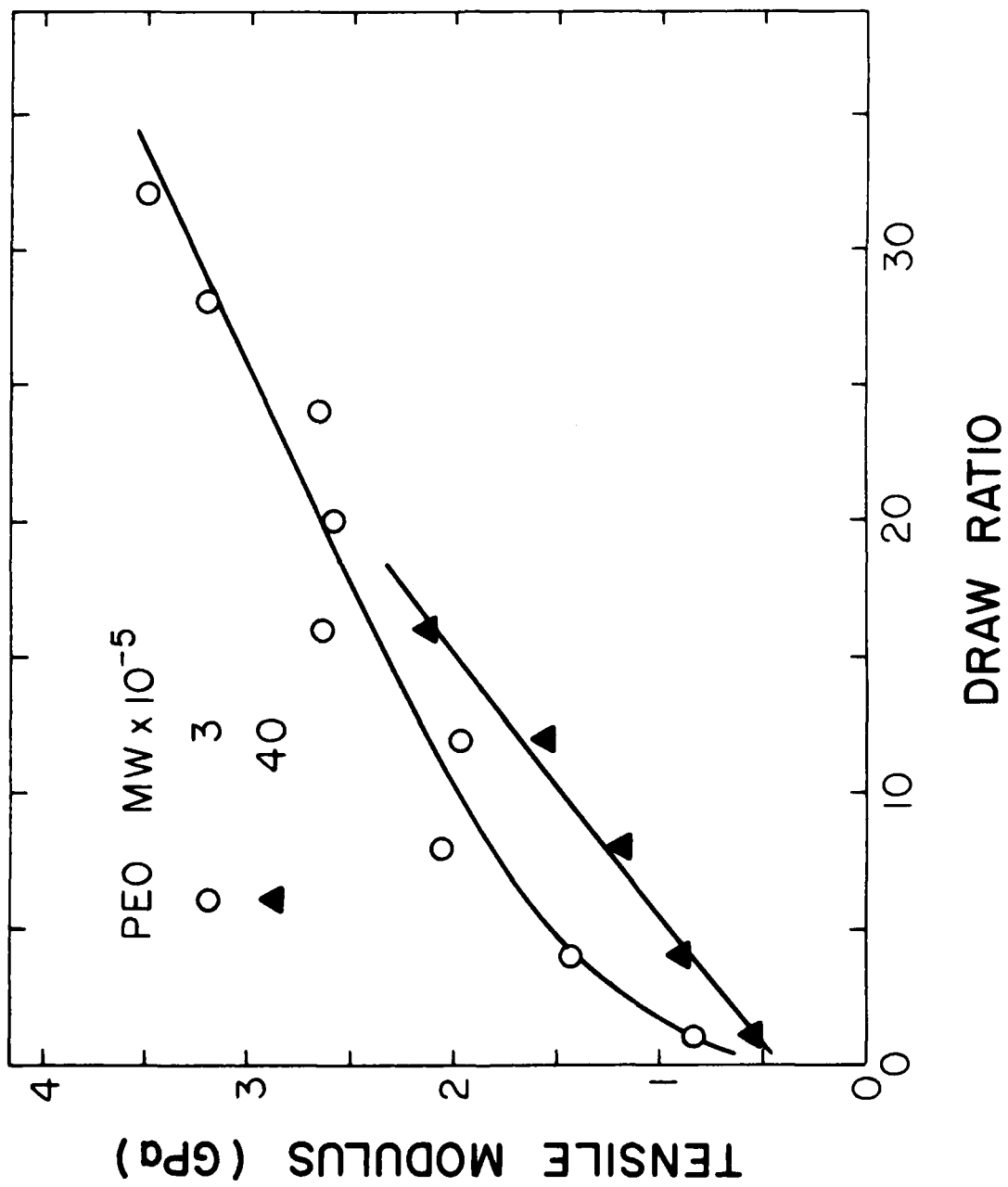


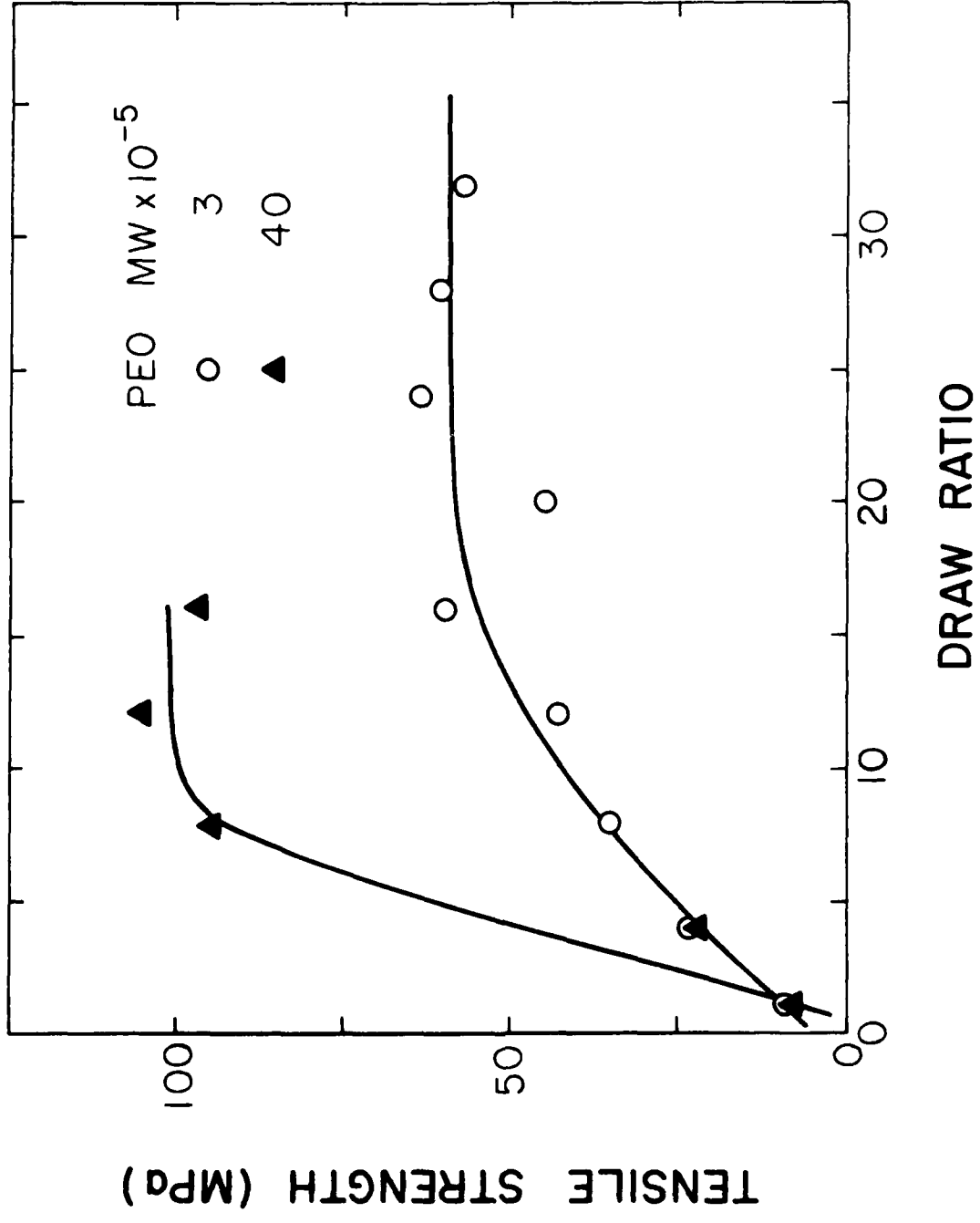
↑ ENDOTHERM

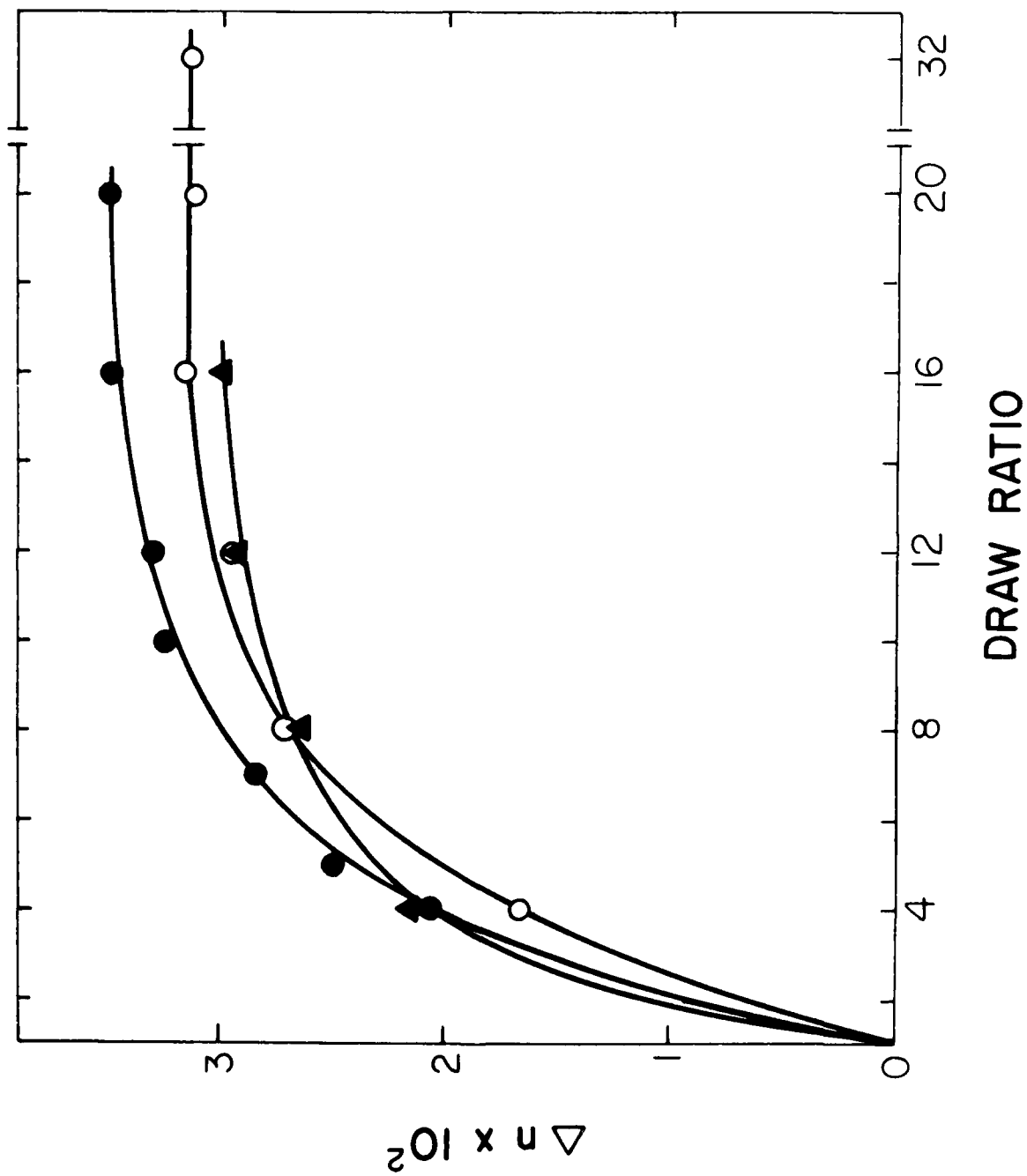
TEMPERATURE (°C)

↑ ENDOTHERM



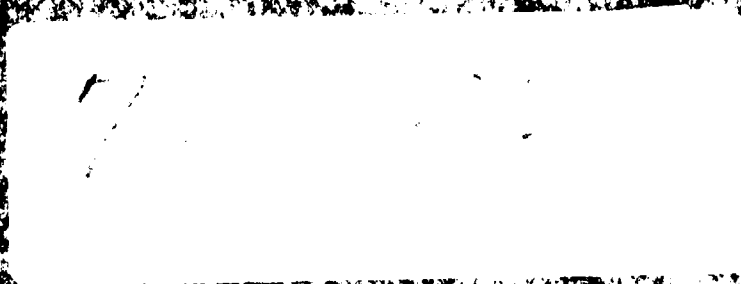






END

FILMED



DTIC